2011-09-10

Multiwavelength Observations Of The Very High Energy Blazar 1es 2344+514

P. T. Reynolds
Cork Institute of Technology

Et. al.

Recommended Citation

Acciari, V. A. et al. (2011) 'MULTIWAVELENGTH OBSERVATIONS OF THE VERY HIGH ENERGY BLAZAR 1ES 2344+514', The Astrophysical Journal, 738(2), p. 169. doi: 10.1088/0004-637X/738/2/169.

The Astrophysical Journal, 738:169 (8pp), 2011 September 10 doi:10.1088/0004-637X/738/2/169

MULTIWAVELENGTH OBSERVATIONS OF THE VERY HIGH ENERGY BLAZAR 1ES 2344+514

V. A. Acciari[1], E. Aliu[2], T. Arlen[3], T. Aune[4], M. Beilicke[5], W. Benbow[1], D. Boltuch[2], V. Bugaev[5], A. Cannon[6], L. Ciupik[7], P. Cogan[8], P. Colin[9], R. Dickherber[5], A. Falcone[10], S. J. Fegan[3], J. P. Finley[11], P. Fortin[12], L. F. Fortson[7], A. Furniss[4], D. Gall[11], G. H. Gillanders[13], J. Grube[6,7], R. Guenette[8], G. Gyuk[7], D. Hanna[8], J. Holder[2], D. Horan[14], C. M. Hui[9], T. B. Humensky[15], A. Imran[16], P. Kaaret[17], N. Karlsson[7], M. Kertzman[18], D. Kieda[9], J. Kildea[1], A. Konopelko[19], H. Krawczynski[5], F. Krennrich[16], M. J. Lang[13], S. LeBohec[9], G. Maier[8], P. Moriarty[20], R. Mukherjee[12], R. A. Ong[3], A. N. Otte[4], D. Pandel[17], J. S. Perkins[1], A. Pichel[21], M. Pohl[16], J. Quinn[6], K. Ragan[8], P. T. Reynolds[22], H. J. Rose[23], M. Schroedter[16], G. H. Sembroski[11], A. W. Smith[24], D. Steele[7], S. P. Swordy[15], M. Theiling[1], J. A. Toner[13], A. Varlotta[11], V. V. Vassiliev[3], S. Vincent[9], R. Wagner[24], S. P. Wakely[15], J. E. Ward[6], T. C. Weekes[1], A. Weinstein[3], T. Weisgarber[15], D. A. Williams[4], S. Wissel[15], M. Wood[3], and B. Zitzer[11]

[1] Fred Lawrence Whipple Observatory, Harvard-Smithsonian Center for Astrophysics, Amado, AZ 85645, USA
[2] Department of Physics and Astronomy and the Bartol Research Institute, University of Delaware, Newark, DE 19716, USA
[3] Department of Physics and Astronomy, University of California, Los Angeles, CA 90095, USA
[4] Santa Cruz Institute for Particle Physics and Department of Physics, University of California, Santa Cruz, CA 95064, USA
[5] Department of Physics, Washington University, St. Louis, MO 63130, USA
[6] School of Physics, University College Dublin, Belfield, Dublin 4, Ireland
[7] Astronomy Department, Adler Planetarium and Astronomy Museum, Chicago, IL 60605, USA; jgrube@adlerplanetarium.org
[8] Physics Department, McGill University, Montreal, QC H3A 2T8, Canada
[9] Physics Department, University of Utah, Salt Lake City, UT 84112, USA
[10] Department of Astronomy and Astrophysics, 525 Davey Lab, Pennsylvania State University, University Park, PA 16802, USA
[11] Department of Physics, Purdue University, West Lafayette, IN 47907, USA
[12] Department of Physics and Astronomy, Barnard College, Columbia University, NY 10027, USA
[13] School of Physics, National University of Ireland, Galway, Ireland
[14] Laboratoire Leprince-Ringuet, Ecole Polytechnique, CNRS/IN2P3, F-91128 Palaiseau, France
[15] Enrico Fermi Institute, University of Chicago, Chicago, IL 60637, USA
[16] Department of Physics and Astronomy, Iowa State University, Ames, IA 50011, USA
[17] Department of Physics and Astronomy, University of Iowa, Van Allen Hall, Iowa City, IA 52242, USA
[18] Department of Physics and Astronomy, DePauw University, Greencastle, IN 46135-0037, USA
[19] Department of Physics, Pittsburg State University, 1701 South Broadway, Pittsburg, KS 66762, USA
[20] Department of Life and Physical Sciences, Galway-Mayo Institute of Technology, Dublin Road, Galway, Ireland
[21] Instituto de Astronomia y Fisica del Espacio, Casilla de Correo 67 - Sucursal 28, (C1428ZAA) Ciudad Autnoma de Buenos Aires, Argentina
[22] Department of Applied Physics and Instrumentation, Cork Institute of Technology, Bishopstown, Cork, Ireland
[23] School of Physics and Astronomy, University of Leeds, Leeds, LS2 9JT, UK
[24] Argonne National Laboratory, 9700 S. Cass Avenue, Argonne, IL 60439, USA
Received 2009 May 11; accepted 2011 June 22; published 2011 August 23

ABSTRACT

Multiwavelength observations of the high-frequency-peaked blazar 1ES 2344+514 were performed from 2007 October to 2008 January. The campaign represents the first contemporaneous data on the object at very high energy (VHE, $E > 100$ GeV) γ-ray, X-ray, and UV energies. Observations with VERITAS in VHE γ-rays yield a strong detection of 20σ with 633 excess events in a total exposure of 18.1 hr live time. A strong VHE γ-ray flare on 2007 December 7 is measured at $F(>300\ \mathrm{GeV}) = (6.76 \pm 0.62) \times 10^{-11}$ photons cm^{-2} s^{-1}, corresponding to 48% of the Crab Nebula flux. Excluding this flaring episode, nightly variability at lower fluxes is observed with a time-averaged mean of $F(>300\ \mathrm{GeV}) = (1.06 \pm 0.09) \times 10^{-11}$ photons cm^{-2} s^{-1} (7.6% of the Crab Nebula flux). The differential photon spectrum between 390 GeV and 8.3 TeV for the time-averaged observations excluding 2007 December 7 is well described by a power law with a photon index of $\Gamma = 2.78 \pm 0.09_{\mathrm{stat}} \pm 0.15_{\mathrm{syst}}$. On the flaring night of 2007 December 7 the measured VHE γ-ray photon index was $\Gamma = 2.43 \pm 0.22_{\mathrm{stat}} \pm 0.15_{\mathrm{syst}}$. Over the full period of VERITAS observations contemporaneous X-ray and UV data were taken with *Swift* and *RXTE*. The measured 2–10 keV flux ranged by a factor of ∼7 during the campaign. On 2007 December 8 the highest ever observed X-ray flux from 1ES 2344+514 was measured by *Swift* X-ray Telescope at a flux of $F(2\text{–}10\ \mathrm{keV}) = (6.28 \pm 0.31) \times 10^{-11}$ erg cm^{-2} s^{-1}. Evidence for a correlation between the X-ray flux and VHE γ-ray flux on nightly timescales is indicated with a Pearson correlation coefficient of $r = 0.60 \pm 0.11$. Contemporaneous spectral energy distributions (SEDs) of 1ES 2344+514 are presented for two distinct flux states. A one-zone synchrotron self-Compton (SSC) model describes both SEDs using parameters consistent with previous SSC modeling of 1ES 2344+514 from non-contemporaneous observations.

Key words: BL Lacertae objects: individual (IES 2344+514)

1. INTRODUCTION

The majority of blazars detected at very high energy (VHE, $E > 100$ GeV) γ-rays are high-frequency-peaked BL Lac objects (HBLs), with currently ∼30 HBLs from a total of ∼40 VHE blazars.[25] The short timescale variability seen in the broadband spectral energy distributions (SEDs) of blazars

[25] The TeVCat catalog of VHE γ-rays sources is available online at: http://tevcat.uchicago.edu.

is explained by highly relativistic plasma jets oriented close to the line of sight (Blandford & Königl 1979). HBLs are blazars exhibiting synchrotron radiation peaking typically at UV to X-ray energies and a second SED component peaking at GeV to TeV energies. Leptonic models (Coppi 1992; Böttcher & Chang 2002; Krawczynski et al. 2004) describe the high-energy (HE) peak as inverse Compton upscattering of low-energy photons by electrons, while hadronic models attribute the emission to proton-induced cascades, synchrotron radiation by protons, pion production in dense clumps of jet plasma, or curvature radiation (Mannheim 1993; Aharonian 2000; Mücke & Protheroe 2001). Detailed multiwavelength studies from optical to γ-ray energies of the temporal and spectral variability of HBLs promise to constrain the physical parameters of the underlying particle distributions, particularly the Doppler factor and magnetic field strength (Tavecchio et al. 1998).

The HBL 1ES 2344+514 was first detected in the Einstein Slew Survey at X-ray energies (0.2–4 keV) and has a redshift of $z = 0.044$ (Elvis et al. 1992; Perlman et al. 1996). VHE γ-ray emission from 1ES 2344+514 was discovered by the Whipple 10 m telescope in energies >350 GeV at a 6.0σ detection level during a 1 day flare on 1995 December 20 (Catanese et al. 1998). X-ray observations of 1ES 2344+514 with *BeppoSAX* revealed variability in the 2–10 keV flux by a factor of ∼2 during a 7 day period in 1996 December (Giommi et al. 2000). 1ES 2344+514 was later observed by *Swift* in 2005 during April, May, and December at a lower flux than in 1996 December (Tramacere et al. 2007). The X-ray spectrum is reasonably well described by an absorbed power law, with photon indices ranging from $\Gamma \approx 1.8$ to 2.3. Marginal evidence for optical variability in 1ES 2344+514 is seen from the sparse data set of two observations in 1998 (Nilsson et al. 1999; Falomo & Kotilainen 1999), six nights in 2000 (Xie et al. 2002), and one observation on 2007 January 12 (Gupta et al. 2008). In the radio band, Very Large Array observations reveal an unusual morphology at arcsec scales for a blazar of two compact high brightness emission regions connected via a diffuse halo, more reminiscent of a radio galaxy (Rector et al. 2003; Giroletti et al. 2004). High-resolution Very Long Baseline Array observations show a well-collimated jet extending ∼10 pc from the core, which then bends 25° and broadens into a cone of ∼35° opening angle. In HE ($0.1 > E < 300$ GeV) γ-rays, 1ES 2344+514 is associated with the source 1FGL J2347.1+5142 from the *Fermi* LAT First Source Catalog (Abdo et al. 2010), detected at a significance of 10.6σ and showing a hard HE γ-ray spectrum of 1.57 ± 0.17 with no indication of HE γ-ray flux variability during the period of 2008 August to 2009 July.

Evidence for long-term VHE γ-ray flux variability in 1ES 2344+514 is seen in observations between 1995 and 2005 by the Whipple 10 m telescope, HEGRA, and MAGIC. The Whipple 10 m γ-ray photon spectrum on the flaring night of 1995 December 20 is best fit by a power law over the energy range 0.8–9 TeV, with a photon index $\Gamma = 2.54 \pm 0.17_{\rm stat} \pm 0.07_{\rm syst}$ (Schroedter et al. 2005). The measured flux $F(>1\ \mathrm{TeV}) = (3.3 \pm 0.7) \times 10^{-11})$ photons cm^{-2} s^{-1} for the flare night is a factor of 1.7 ± 0.3 higher than the Crab Nebula flux. Excluding 1995 December 20, the time-averaged Whipple 10 m data between 1995 and 1997 yielded a marginal 4σ detection at a significantly lower flux level, corresponding to ∼10% of the Crab Nebula flux (Catanese et al. 1998). Further VHE γ-ray observations of 1ES 2344+514 with HEGRA in 1997, 1998, and 2002 resulted in a 4.4σ detection in a low flux level state of (3.3 ± 1.0)% of the Crab Nebula flux (Aharonian et al. 2004). Observations in 1995 with TACTIC above 1.5 TeV in 2004 and 2005 yielded a weakly constraining flux upper limit near the Whipple 10 m detection flux level (Godambe et al. 2007). In 2005 August to 2006 January, the MAGIC telescope measured a time-averaged photon spectrum between 0.14 and 5.4 TeV at a low flux of 5% of the Crab Nebula flux characterized by a power law with $\Gamma = 2.95 \pm 0.12_{\rm stat} \pm 0.20_{\rm syst}$ (Albert et al. 2007). This article presents the first multiwavelength campaign on 1ES 2344+514, with contemporaneous UV, X-ray, and VHE γ-ray observations over a several month long period.

2. VERITAS OBSERVATIONS

VERITAS is an array of four 12 m diameter imaging atmospheric Cherenkov telescopes located at the Fred Lawrence Whipple Observatory in Southern Arizona (Weekes et al. 2002). Each VERITAS camera contains 499 pixels (0.°15 diameter) and has a field of view of 3.°5. VERITAS is sensitive over an energy range of ∼100 GeV to ∼30 TeV with an energy resolution of 15%–20% and an angular resolution (68% containment) of less than 0.°14 per event (Acciari et al. 2008). VERITAS can detect VHE γ-ray fluxes of 5% and 1% of the Crab Nebula flux at the 5σ level in <2.5 and <50 hr, respectively.

The VERITAS observations of 1ES 2344+514 presented here were taken on 37 nights between 2007 October 4 and 2008 January 11. After applying quality-selection criteria, the total exposure is 18.1 hr live time. Data-quality selection requires clear atmospheric conditions, based on infrared sky temperature measurements, and normal hardware operation. During each night, the quality-selected data ranged from 0.3 to 2.7 hr live time. The zenith angle of observations ranges from 19° to 48°, with a mean of 28°. All data were taken during moon-less periods in *wobble* mode with pointings of 0.°5 from the blazar alternating from north, south, east, and west directions to enable simultaneous background estimation (Aharonian et al. 2001).

Data reduction followed the methods described in Acciari et al. (2008). Signals in each event are first calibrated (Holder et al. 2006), and the images are parameterized (Hillas 1985). The γ-ray direction and air shower impact parameter on the ground are then reconstructed using stereoscopic techniques (Hofmann et al. 1999; Krawczynski et al. 2006). The background of cosmic rays is rejected with a very high efficiency using event-by-event cuts on the arrival direction (θ^2), mean scaled width and length, integrated charge (*size*), and location of the image centroids in the camera (*distance*). The cuts applied here are optimized a priori for a source strength of 10% of the Crab Nebula flux and a similar photon index to the Crab Nebula. The energy of each event is reconstructed using lookup tables from Monte Carlo simulations of γ-rays (Acciari et al. 2008). Results from two independent VERITAS analysis packages (Daniel et al. 2007) yield results consistent with those presented here.

A total of 1275 on-source and 4494 off-source events were measured, with an on–off normalization of $\alpha = 0.143$. This corresponds to a total excess of 632 events from the direction of 1ES 2344+514. The statistical significance of this excess is 20.2 standard deviations (σ). Figure 1 shows the θ^2 distribution of the total data set, which is the squared angular distance between the reconstructed event direction and the nominal source position. The shape of the excess is consistent with a simulated point source for VERITAS.

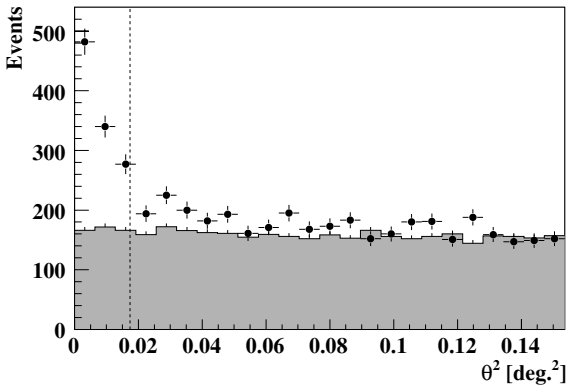

Figure 1. Distribution of θ^2 for on-source events (points) and normalized off-source events (shaded region) from observations of 1ES 2344+514. The dashed line represents the applied cut on the θ^2 parameter.

3. *RXTE* OBSERVATIONS

The X-ray satellite mission *RXTE* (Bradt et al. 1993) observed 1ES 2344+514 between 2007 October 7 and 2008 January 11 (ObsID 93132). Data are presented from Proportional Counter Unit 2 (PCU 2) of the Proportional Counter Array (PCA) instrument (Jahoda et al. 1996) since for nearly all observations the other PCUs were not in operation. The 52 nightly PCA observations were taken in snapshots ranging from 0.11 to 1.00 hr live time and are listed in Table 1. Data reduction is performed with the *HEAsoft* 6.5 package. Only the top layer (X1L and X1R) signal is used. The data are filtered following the standard criteria advised by the NASA Guest Observer Facility. Background data are parameterized with the *pcabackest* tool using the most recent model for faint sources. The photon spectrum of each observation is extracted using the *saextrct* tool. Response matrices are generated using *pcarsp* with the latest calibration files.

4. *SWIFT* OBSERVATIONS

Swift (Gehrels et al. 2004) Target of Opportunity observations of 1ES 2344+514 from 2007 October 27 to 2008 January 1 were triggered by the VERITAS detection. The *Swift* data set consists of eight snapshot observations of 10–45 minute duration each, as listed in Table 1. All *Swift* X-ray Telescope (XRT) data (Burrows et al. 2005) are reduced using the *HEAsoft* 6.5 package. Event files are calibrated and cleaned following the standard filtering criteria using the *xrtpipeline* task and applying the most recent *Swift* XRT calibration files. All data were taken in photon counting (PC) mode, with grades 0–12 selected over the energy range 0.3–10 keV. Due to photon pile-up in the core of the point-spread function (PSF) at count rates >0.5 counts s^{-1} (PC mode), the source events are extracted from an annular region with inner radius ranging from 2 to 6 pixels and an outer radius of 30 pixels (47.2 arcsec). Background counts are extracted from a 40 pixel radius circle in a source-free region. Ancillary response files are generated using the *xrtmkarf* task, with corrections applied for the PSF losses and CCD defects. The latest response matrix from the XRT calibration files is applied. To ensure valid χ^2 minimization statistics during spectral fitting, the extracted XRT energy spectra are rebinned to contain a minimum of 30 counts in each bin.

Swift Ultraviolet and Optical Telescope (UVOT) observations were taken in the photometric bands of *UVW1*, *UVM2*, and *UVW2* (Poole et al. 2008). The *uvotsource* tool is used to extract counts, correct for coincidence losses, apply background subtraction, and calculate the source flux. The standard 5 arcsec radius source aperture is used, with a 20 arcsec background region. The source fluxes are dereddened using the interstellar extinction curve in Fitzpatrick (1999). In the UV filters only a low level of host galaxy flux is evident (Tramacere et al. 2007), so no corrections are needed. The uncertainty in PSF variations with time is fixed for this analysis at 15%. Observations were taken with just one UV filter during each pointing, and only *UVM2* data were taken on multiple nights. Within the conservative errors, no variability is seen between the four *UVM2* filter observations.

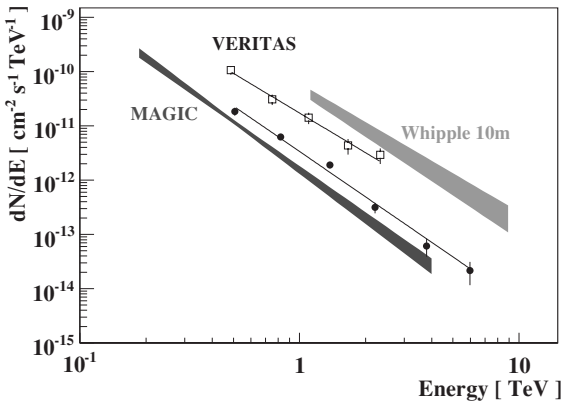

Figure 2. Differential photon spectrum of VHE γ-rays for 1ES 2344+514. The circles represent the time-averaged VERITAS data from 2007 October to 2008 January, excluding the bright flare on 2007 December 7. The open squares represent VERITAS data from the flare night. Shown for comparison are the 68% confidence intervals for the best-fit power-law models to 1ES 2344+514 data from MAGIC (dark gray band) in 2005 August to 2006 January (Albert et al. 2007), and from the Whipple 10 m (light gray band) during a high-flux state on 1995 December 20 (Schroedter et al. 2005).

5. SPECTRAL ANALYSIS

The VERITAS differential photon spectrum over the energy range of 390 GeV to 8.3 TeV for the time-averaged data excluding a strong flaring night on 2007 December 7 is shown in Figure 2. A power-law model fit to the data is best described by the form $dN/dE = F_\circ \cdot (E/1\,\mathrm{TeV})^{-\Gamma}$ yielding a χ^2/dof of 8.39/4 for a flux normalization constant of $F_\circ = (3.38 \pm 0.23_{\mathrm{stat}} \pm 0.70_{\mathrm{syst}}) \times 10^{-12}$ photons $\mathrm{cm}^{-2}\ \mathrm{s}^{-1}\ \mathrm{TeV}^{-1}$ and a photon index of $\Gamma = 2.78 \pm 0.09_{\mathrm{stat}} \pm 0.15_{\mathrm{syst}}$. A fit to a power law with an exponential cutoff model, which contains one additional degree of freedom, does not yield a significantly better fit. On 2007 December 7 the weather conditions were affected by moving cloud coverage, so the observations do not pass the standard data-quality criteria. However, online analysis showed that the source was in the most active state yet observed. We therefore include these data and increase the systematic uncertainties in flux and spectral shape. Conservative systematic uncertainties in the flux of 30% and photon index of 0.2 are determined, based on the results of observations of the Crab Nebula taken in similarly variable conditions. The VHE γ-ray spectrum from the high-flux night is well described by a power law (χ^2/dof of 1.27/3) with a slightly harder photon index $\Gamma = 2.43 \pm 0.22_{\mathrm{stat}} \pm 0.2_{\mathrm{syst}}$ and a higher flux normalization of $F_\circ = (17.3 \pm 1.92_{\mathrm{stat}} \pm 5.19_{\mathrm{syst}}) \times 10^{-12}$ photons $\mathrm{cm}^{-2}\ \mathrm{s}^{-1}\ \mathrm{TeV}^{-1}$.

The best-fit results presented here are tested with a dedicated Monte Carlo study, which explores the uncertainty ranges for the two measured spectra. In the Monte Carlo study photons are selected from a power-law distribution matching the measured

Table 1
Best-fit Spectral Parameters for the *Swift* XRT and *RXTE* PCA Data

Date	Start (hr:min UT)	Exp. (ks)	Γ	$K_{1\,\mathrm{keV}}$ (10^{-2} photons cm^{-2} s^{-1} keV^{-1})	χ^2_r/dof	F(2–10 keV) (10^{-11} erg cm^{-2} s^{-1})
Swift XRT						
2007 Oct 27	10:24	2.66	2.33 ± 0.05	0.62 ± 0.03	1.11/36	0.96 ± 0.06
2007 Nov 3	03:02	1.97	2.32 ± 0.06	0.87 ± 0.04	1.02/27	1.37 ± 0.09
2007 Nov 10	05:03	0.63	2.26 ± 0.13	1.26 ± 0.10	0.69/8	2.18 ± 0.31
2007 Nov 17	02:28	1.65	2.16 ± 0.06	0.76 ± 0.04	0.71/23	1.51 ± 0.14
2007 Nov 30	03:46	1.85	2.10 ± 0.07	0.91 ± 0.05	1.51/23	1.99 ± 0.14
2007 Dec 8	03:20	2.22	1.97 ± 0.05	2.37 ± 0.10	0.77/33	6.28 ± 0.31
2007 Dec 22	04:28	2.23	2.18 ± 0.05	1.00 ± 0.04	1.12/36	1.93 ± 0.13
2008 Jan 1	00:35	1.37	2.10 ± 0.08	1.26 ± 0.07	1.07/18	2.72 ± 0.17
RXTE PCA						
2007 Oct 7	06:03	2.56	2.48 ± 0.26	0.75 ± 0.35	0.52/38	0.95 ± 0.26
2007 Oct 8	06:56	2.88	2.65 ± 0.20	1.24 ± 0.38	0.58/38	1.24 ± 0.15
2007 Oct 9	06:14	2.80	2.31 ± 0.13	1.04 ± 0.23	0.54/38	1.66 ± 0.10
2007 Oct 10	05:53	2.67	2.17 ± 0.12	0.89 ± 0.19	0.47/38	1.76 ± 0.14
2007 Oct 11	03:42	2.16	2.57 ± 0.15	1.65 ± 0.40	0.42/38	1.85 ± 0.11
2007 Oct 12	03:14	0.21	2.57 ± 0.19	1.34 ± 0.41	0.66/38	1.48 ± 0.15
2007 Oct 13	04:52	2.02	2.26 ± 0.13	1.11 ± 0.24	0.63/38	1.92 ± 0.15
2007 Oct 14	02:17	1.86	2.39 ± 0.12	1.63 ± 0.33	0.62/38	2.35 ± 0.14
2007 Oct 15	03:56	1.50	2.49 ± 0.16	1.61 ± 0.41	0.53/38	2.02 ± 0.20
2007 Oct 16	04:35	1.84	2.25 ± 0.18	0.80 ± 0.27	0.53/38	1.41 ± 0.24
2007 Oct 19	07:09	3.62	2.42 ± 0.14	1.02 ± 0.23	0.51/38	1.39 ± 0.13
2007 Oct 20	08:18	3.15	2.61 ± 0.15	1.51 ± 0.35	0.59/38	1.59 ± 0.12
2007 Oct 21	07:57	3.49	2.36 ± 0.16	0.81 ± 0.23	0.56/38	1.22 ± 0.11
2007 Nov 1	03:06	2.59	2.19 ± 0.15	0.73 ± 0.21	0.79/38	1.40 ± 0.13
2007 Nov 2	05:53	1.39	2.41 ± 0.18	1.25 ± 0.37	0.62/38	1.73 ± 0.16
2007 Nov 3	07:06	2.37	2.72 ± 0.19	1.65 ± 0.48	0.53/38	1.50 ± 0.14
2007 Nov 4	04:56	2.85	2.19 ± 0.14	0.75 ± 0.20	0.50/38	1.43 ± 0.11
2007 Nov 5	06:35	0.80	2.20 ± 0.29	0.68 ± 0.40	0.64/38	1.28 ± 0.45
2007 Nov 6	04:02	2.48	2.23 ± 0.11	1.10 ± 0.21	0.82/38	2.00 ± 0.11
2007 Nov 7	06:36	0.31	2.43 ± 0.12	1.28 ± 0.25	0.49/38	1.75 ± 0.09
2007 Nov 8	07:52	2.96	2.20 ± 0.10	1.10 ± 0.18	0.57/38	2.07 ± 0.11
2007 Nov 9	07:35	2.40	2.10 ± 0.09	1.16 ± 0.17	0.59/38	2.53 ± 0.12
2007 Nov 10	03:50	2.53	2.13 ± 0.08	1.41 ± 0.18	0.33/38	2.94 ± 0.09
2007 Nov 11	01:49	2.27	2.16 ± 0.08	1.50 ± 0.20	0.63/38	3.02 ± 0.13
2007 Nov 12	04:31	2.51	2.23 ± 0.13	0.91 ± 0.21	0.54/38	1.65 ± 0.16
2007 Nov 13	02:30	2.30	2.11 ± 0.09	1.19 ± 0.18	0.71/38	2.57 ± 0.13
2007 Nov 14	03:37	2.40	2.22 ± 0.11	1.15 ± 0.21	0.55/38	2.12 ± 0.10
2007 Nov 15	03:10	2.34	2.50 ± 0.16	1.31 ± 0.33	0.60/38	1.61 ± 0.15
2007 Nov 30	02:20	0.37	2.44 ± 0.26	1.91 ± 0.81	0.74/38	2.54 ± 0.37
2007 Dec 1	01:51	0.50	2.59 ± 0.33	1.62 ± 0.84	0.38/38	1.76 ± 0.46
2007 Dec 2	05:03	0.58	2.23 ± 0.18	1.48 ± 0.43	0.72/38	2.65 ± 0.25
2007 Dec 4	02:31	0.40	2.10 ± 0.19	1.32 ± 0.42	0.61/38	2.87 ± 0.39
2007 Dec 5	02:11	1.79	2.01 ± 0.05	2.15 ± 0.19	0.81/38	5.37 ± 0.15
2007 Dec 6	03:28	1.57	2.06 ± 0.06	1.99 ± 0.22	0.69/38	4.63 ± 0.11
2007 Dec 10	02:18	2.03	1.94 ± 0.06	1.39 ± 0.15	0.90/38	3.90 ± 0.10
2007 Dec 11	02:50	1.82	1.87 ± 0.04	1.97 ± 0.15	0.62/38	6.10 ± 0.11
2007 Dec 13	03:38	3.39	1.86 ± 0.04	1.54 ± 0.10	0.67/38	4.85 ± 0.07
2007 Dec 12	05:41	1.23	1.97 ± 0.06	1.96 ± 0.21	0.46/38	5.20 ± 0.13
2007 Dec 14	04:35	3.33	2.08 ± 0.06	1.53 ± 0.15	0.65/38	3.42 ± 0.09
2007 Dec 15	04:53	0.86	2.17 ± 0.13	1.57 ± 0.33	0.91/38	3.10 ± 0.23
2007 Dec 28	03:46	1.06	2.14 ± 0.11	1.48 ± 0.28	0.72/38	3.06 ± 0.17
2007 Dec 29	04:53	1.17	1.96 ± 0.15	0.69 ± 0.22	0.47/38	1.86 ± 0.23
2007 Dec 30	04:25	0.88	1.91 ± 0.09	1.40 ± 0.22	0.56/38	4.04 ± 0.22
2008 Jan 1	01:52	0.86	2.06 ± 0.11	1.43 ± 0.27	0.85/38	3.30 ± 0.15
2008 Jan 2	02:26	2.66	2.12 ± 0.07	1.40 ± 0.17	0.53/38	2.96 ± 0.11
2008 Jan 3	03:34	2.91	1.97 ± 0.06	1.23 ± 0.13	0.67/38	3.26 ± 0.10
2008 Jan 4	01:53	1.71	2.06 ± 0.13	0.87 ± 0.20	0.65/38	2.03 ± 0.12
2008 Jan 5	02:35	2.83	1.97 ± 0.07	1.02 ± 0.13	0.51/38	2.71 ± 0.11
2008 Jan 6	02:08	2.75	2.31 ± 0.12	1.08 ± 0.22	0.41/38	1.76 ± 0.11
2008 Jan 7	03:48	1.98	2.33 ± 0.14	1.16 ± 0.27	0.68/38	1.83 ± 0.12
2008 Jan 10	02:23	1.50	2.25 ± 0.10	1.78 ± 0.29	0.52/38	3.12 ± 0.14
2008 Jan 11	03:24	2.77	2.12 ± 0.07	1.53 ± 0.17	0.74/38	3.25 ± 0.10

distribution convolved with the effective area as a function of energy. The selected photon energies are then smeared with a Gaussian corresponding to the energy resolution of ∼15% at these energies. The number of photons selected is matched to the observed number of photons with a Poisson scatter. Five million synthetic photon spectra are created using similar binning to the original spectra, and the best-fit power-law index and normalization parameters are extracted for each synthetic spectrum providing dense coverage of the parameter space. The Monte Carlo mean value and one-dimensional standard deviation of the power-law parameters are consistent with the best-fit parameters of the measured spectra. For the time-averaged spectrum excluding the flaring night of 2007 December 7, the Monte Carlo study yields a mean value and 1σ error for the flux normalization of $F_{\circ,\mathrm{MC}} = (3.35 \pm 0.30) \times 10^{-12}$ photons cm^{-2} s^{-1} TeV^{-1} and for the photon index of $\Gamma_{\mathrm{MC}} = 2.76 \pm 0.15$. For the high flux 2007 December 7 spectrum, the Monte Carlo study yields $F_{\circ,\mathrm{MC}} = (17.3 \pm 2.67) \times 10^{-12}$ ph cm^{-2} s^{-1} TeV^{-1} and $\Gamma_{\mathrm{MC}} = 2.40 \pm 0.28$.

Previous VHE γ-ray observations of 1ES 2344+514 with the MAGIC telescope between 2005 August and 2006 January measured a constant flux at a slightly lower level than the time-averaged (flare excluded) flux measured here, and a consistent photon index of $\Gamma = 2.95 \pm 0.12_{\mathrm{stat.}} \pm 0.2_{\mathrm{syst.}}$ (Albert et al. 2007). The high-flux VHE γ-ray photon spectrum measured by the Whipple 10 m on 1995 December 20 with a photon index of $\Gamma = 2.54 \pm 0.17_{\mathrm{stat}} \pm 0.07_{\mathrm{syst}}$ (Schroedter et al. 2005) is marginally harder than the low flux spectrum and agrees with the high-flux spectrum measured here. The VHE observed γ-ray spectral shape and intensity are modified by absorption from pair production interactions with the infrared component of the extragalactic background light (EBL; Gould & Schréder 1967). Using the redshift $z = 0.044$ for 1ES 2344+514, we calculate a de-absorbed spectrum based on the EBL model of Franceschini et al. (2008), yielding intrinsic photon indices for the VERITAS low and high-flux states of $\Gamma_{\mathrm{int,low}} \approx 2.5$ and $\Gamma_{\mathrm{int,high}} \approx 2.1$, respectively.

X-ray spectral analysis of the *Swift* XRT and *RXTE* PCA data is performed with *XSPEC* 12.4. An absorbed power-law model, including the *phabs* model for the photoelectric absorption, is fit to each spectrum. First, a joint fit of the eight *Swift* XRTs over the energy range 0.4–10 keV using a tied column density N_{H} and each spectrum having a varying photon index and normalization is compared to a joint fit with a fixed Galactic column density $N_{\mathrm{H,Gal}}$ of 1.50×10^{21} cm^{-2} (Kalberla et al. 2005). The joint fit with tied N_{H} yields a best-fit N_{H} of $(2.06 \pm 0.13) \times 10^{21}$ cm^{-2}, with a reduced χ^2 of 1.03 for 203 degrees of freedom (dof) and chance probability for larger chi-squared statistics (null hypothesis) of 37%. The alternative joint fit with the fixed Galactic column density $N_{\mathrm{H,Gal}}$ yields a higher reduced χ^2 of 1.13 for 204 dof and null hypothesis of 9.2%. The best-fit N_{H} is then used in the absorbed power-law model for the *RXTE* PCA spectra, which are mostly unaffected by absorption due to the 3–20 keV energy range, and for all *Swift* XRT results presented here. Figure 3 shows *Swift* XRT (0.4–10 keV) and *RXTE* PCA (3–20 keV) spectra from example moderate-flux and high-flux observations. The ratio in each energy bin of the data to the absorbed power-law model is shown for the example spectra, with the full list of reduced χ^2 values per dof for each observation listed in Table 1. The model describes well the spectra, yielding an average chance probability for larger chi-squared statistics of 37% and 51% for the *Swift* XRT and *RXTE* PCA data, respectively. The measured *Swift* XRT 0.4–10 keV photon indices range from $\Gamma = 2.33 \pm 0.05$ to $\Gamma = 1.97 \pm 0.05$ for observations differing in 2–10 keV integrated flux by a factor of 6.54 ± 0.52. These results are consistent with the *BeppoSAX* 0.5–10 keV photon indices of $\Gamma \approx 1.8$–2.3 at similar flux levels for an absorbed power-law model with fixed Galactic column density (Giommi et al. 2000). Detailed results from the nightly *RXTE* PCA and *Swift* XRT spectra focusing on the connection between the significant X-ray spectral and flux variability are presented in the following section.

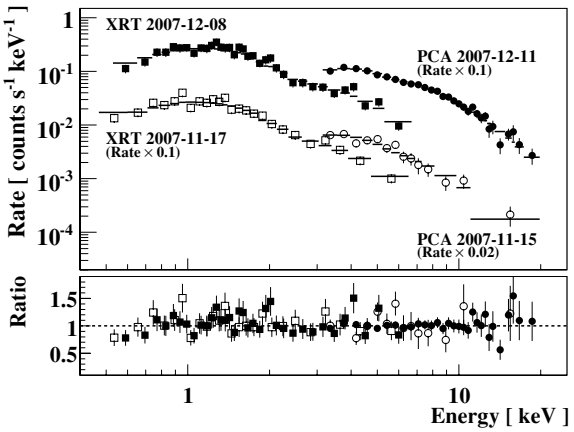

Figure 3. X-ray spectrum of 1ES 2344+514 from *Swift* XRT and *RXTE* PCA observations. Shown in the top panel are example moderate-flux and high-flux spectra identified in the plot by instrument and observation date. The differential rates are scaled in three cases for viewing purposes. For each energy bin, the statistical significance is $>3\sigma$, and the horizontal line represents the best-fit forward folded absorbed power-law model. The bottom panel shows the ratio of the data and model values.

6. LIGHT CURVES

The nightly VHE γ-ray and X-ray light curve of 1ES 2344+514 from VERITAS, *RXTE* PCA, and *Swift* XRT is shown in Figure 4. A strong VHE γ-ray flare is seen on 2007 December 7 (54441.12 MJD) at an integrated flux $F(>300\ \mathrm{GeV}) = (6.8 \pm 0.6) \times 10^{-11}$ cm^{-2} s^{-1}, corresponding to 48% of the Crab Nebula flux. The measured increase in flux of a factor of 1.9 ± 0.5 between the previous night and the flare night shows the first clear evidence of ∼day timescale VHE γ-ray variability from 1ES 2344+514 since the Whipple 10 m discovery of VHE γ-ray emission in 1995 (Catanese et al. 1998). Excluding the 2007 December 7 flaring event, the average $F(E>300\ \mathrm{GeV})$ is $(1.1 \pm 0.1) \times 10^{-11}$ photons cm^{-2} s^{-1}, corresponding to 7.6% of the Crab Nebula flux. A fit to a constant flux excluding the flaring night is rejected with a chance probability of 7.2×10^{-8}, indicating significant low-level variability. A measure of the integrated level of flux variability is the fractional root-mean-square variability amplitude F_{var} (Vaughan et al. 2003). For the full VERITAS data set of nightly exposures a high level of variability $F_{\mathrm{var}} = (75 \pm 10)\%$ is implied. Excluding the flare night, a still significant $F_{\mathrm{var}} = (34 \pm 16)\%$ is determined. Searches for short-term flux variations within each of the nightly observations showed no significant variability.

Figure 4 (lower panels) shows the 2–10 keV flux and photon index Γ measured over 3–20 keV from *RXTE* PCA and 0.4–10 keV from *Swift* XRT data. The X-ray flux is shown to be highly variable throughout the campaign, with $F_{\mathrm{var}} = (51 \pm 1)\%$. In 2007 December, large amplitude flaring is evident with flux doubling timescales of ∼1 day. A 2–10 keV flux of $(6.3 \pm 0.3) \times 10^{-11}$ erg cm^{-2} s^{-1} is seen from the *Swift* XRT data

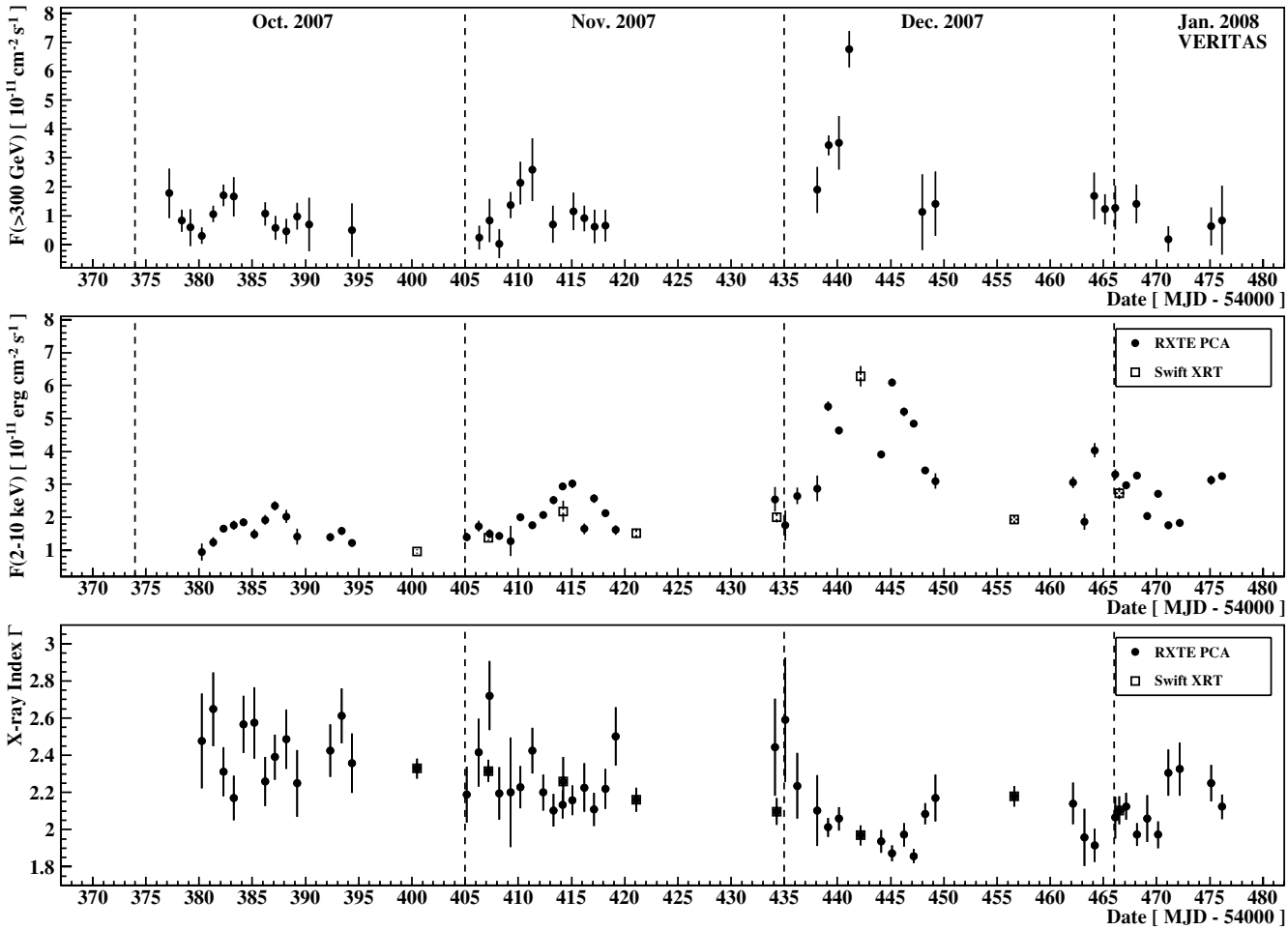

Figure 4. VHE γ-ray and X-ray light curve of 1ES 2344+514. Shown in the top panel are VERITAS $F(>300$ GeV) nightly fluxes. The middle panel shows the 2–10 keV fluxes from observations with *RXTE* PCA (circles) and *Swift* XRT (open squares). The bottom panel shows X-ray photon indices from the best-fit absorbed power-law model.

on 2007 December 8, representing the highest X-ray flux ever measured for 1ES 2344+514. Analysis of all subsequent X-ray data of 1ES 2344+514, which currently consists solely of *Swift* XRT observations, shows a 2–10 keV flux consistent with the lowest flux measurements presented here. Detailed results from the more recent *Swift* XRT data set are beyond the scope of this publication, but automated count rate light curves are publicly available.[26]

X-ray spectral variability between flaring nights is investigated by plotting the X-ray photon index Γ versus the 2–10 keV flux, shown in Figure 5. A logarithmic correlation of decreasing photon index with increasing flux is suggested from a power-law fit to the *RXTE* PCA and *Swift* XRT data with a χ^2/dof probability of 0.14 and 0.70 compared to 7.9×10^{-20} and 3.3×10^{-4} for a constant photon index, respectively. Due to the lack of significant curvature in the X-ray spectrum, the peak energy $E_{\rm p}$ for a $\nu F(\nu)$ SED representation is largely unconstrained. A comparison of the photon indices from the *Swift* XRT and *RXTE* PCA spectra restricted to the overlapping energy range of 3–10 keV is limited by the low number of energy bins above 3 keV, so a study of the systematically higher *RXTE* PCA (3–20 keV) photon indices compared with the *Swift* XRT (0.4–10 keV) photon indices at similar flux levels is inconclusive. Furthermore, the

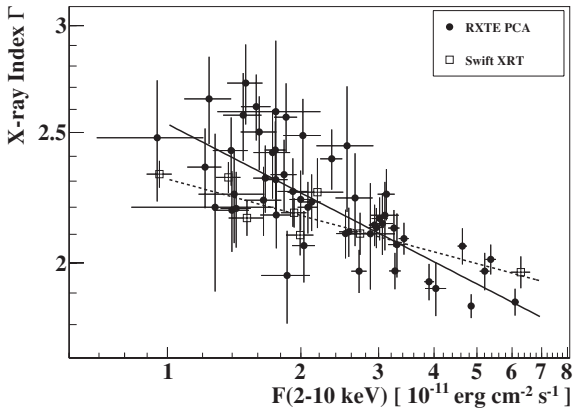

Figure 5. X-ray photon index vs. 2–10 keV flux from *RXTE* PCA (circles) and *Swift* XRT (open squares) data on a log–log scale. The best-fit power law for the *RXTE* PCA (3–20 keV) data is represented by a solid line and for *Swift* XRT (0.4–10 keV) with a dashed line.

lack of purely simultaneous *RXTE* PCA and *Swift* XRT data does not allow for a detailed study of joint fits from 0.4–20 keV. Even during the bright flaring events in 2007 December, the *RXTE* PCA spectra from 3 to 20 keV show no sign of curvature, with measured photon indices of $\sim$1.9. For these high-flux states the implied peak energy $E_{\rm p} \leqslant 10$ keV agrees with the

[26] The *Swift* XRT Monitoring of *Fermi* LAT Sources of Interest is available online at: http://www.swift.psu.edu/monitoring/.

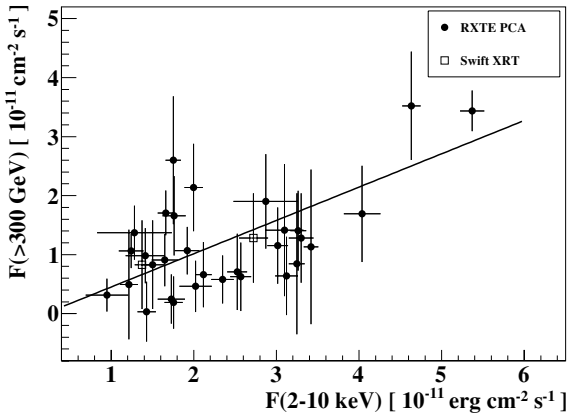

Figure 6. VERITAS γ-ray flux $F(>300$ GeV) vs. X-ray 2–10 keV flux from nights with *RXTE* PCA (circles) and *Swift* XRT (open squares) data. A linear fit to the data is represented by the solid line.

estimated peak energies derived from *BeppoSAX* observations in 1998 (Giommi et al. 2000).

Figure 6 shows the VERITAS flux $F(>300$ GeV) versus *RXTE* PCA and *Swift* XRT 2–10 keV fluxes for nights with observations in both energy bands. A Pearson coefficient of $r = 0.60 \pm 0.11$ is calculated for the VHE γ-ray to X-ray flux points, suggestive of correlated variability. The best-fit linear model yields a slope of 0.56 ± 0.08 with a fit probability of 0.14. For the highest measured X-ray fluxes in 2007 December the weather conditions at the VERITAS site were poor, which excludes these nightly fluxes from Figure 6. Due to the sparse data sampling, a search for lags between the VHE γ-ray and X-ray emission is not investigated here.

7. DISCUSSION

The broadband SED of HBLs is often modeled within a synchrotron self-Compton (SSC) framework. Simple one-zone SSC models typically predict correlated X-ray and VHE γ-ray variability from the underlying electron distribution. Figure 7 shows a one-zone SSC model calculation (Krawczynski et al. 2004) to the SED of 1ES 2344+514 for illustration purposes in two flux states. A high-flux SED is constructed from the VERITAS photon spectrum in 2007 December 7 and *Swift* UVOT and XRT data on 2007 December 8. The time-averaged (flare excluded) VERITAS data are combined with *Swift* and *RXTE* PCA spectra on 2008 January 1 when the object was at a moderate X-ray flux state with respect to the full campaign. Shown also in Figure 7 are the non-contemporaneous MAGIC data from 2005 in a low-flux state and the flaring Whipple 10 m data from 1995 December 20. Also shown for reference is the *Fermi* LAT spectrum from 2008 August to 2009 July in a non-variable low-flux state. Each model curve for the broadband data contemporaneous with the VERITAS data represents the intrinsic source radiation, and all VHE γ-ray spectra are corrected for absorption by the EBL (Franceschini et al. 2008). The SSC model input parameters for the low (high, when different) states are a Doppler factor $\delta = 13$ (20), magnetic field $= 0.09$ G (0.03 G), emission radius $= 10^{16}$ cm, electron density $= 0.05$ ergs cm^{-3}, and a broken power-law electron spectrum with low energies between 10^8 eV and $10^{11.3}$ eV ($10^{11.4}$ eV) with spectral index $n_1 = 2.5$ (2.3), and above the cutoff energy with index $n_1 = 3.2$ and highest energy of 10^{12} eV.

The light crossing time $\tau = R/(c \times \delta) \approx 5$ hr for the high-flux state with a Doppler factor $\delta = 20$ is consistent with the ~hour timescale X-ray variability seen from 1ES 2344+514 with *BeppoSAX* on 1996 December 7 (Giommi et al. 2000). Further hourly X-ray variability in 1ES 2344+514 could not be confirmed in this work due to the short (<hour) exposures with *Swift* and *RXTE* and moderate event statistics. In addition to the low- and high-flux state modeling from data in 2007 October to 2008 January, the same SSC model was applied to non-contemporaneous low- and high-flux states derived from *BeppoSAX*, MAGIC, and Whipple 10 m spectra (Albert et al. 2007). A reasonable agreement between model parameters, such as Doppler factors ~10–20 and a magnetic field ~0.03–0.3 G,

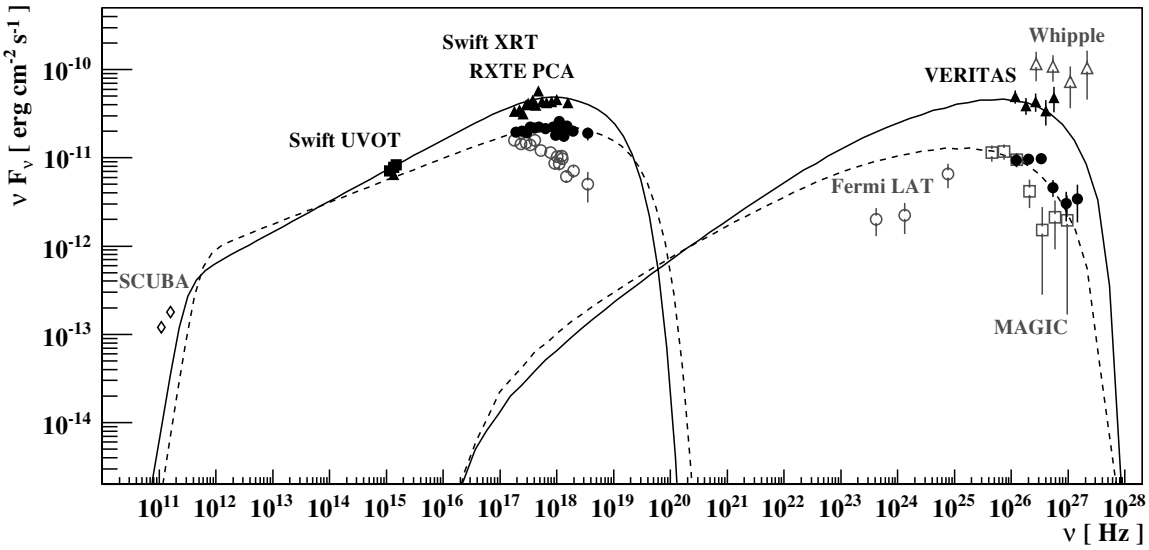

Figure 7. Spectral energy distribution of 1ES 2344+514. The high-flux spectra (triangles) are from VERITAS data on 2007 December 7 and *Swift* UVOT and XRT data on 2007 December 8. The time-averaged VERITAS spectrum and moderate-flux level X-ray spectrum from *Swift* XRT and *RXTE* PCA data on 2008 January 1 are represented by circles. An example low flux X-ray spectrum (open circles) is from 2007 November 3. Non-contemporaneous VHE γ-ray spectra are shown from MAGIC data in 2005 August–December (open squares) and from Whipple 10 m data on the flare night of 1995 December 20 (open triangles). All VHE γ-ray spectra are corrected for absorption by the extragalactic background light (Franceschini et al. 2008). Archival millimeter fluxes (open diamonds) are from SCUBA data (Stevens & Gear 1999). The non-contemporaneous *Fermi* LAT spectrum from the 1FGL catalog is represented by open circles (Abdo et al. 2010). The broadband curves are from synchrotron self-Compton (SSC) modeling to the contemporaneous data (Krawczynski et al. 2004).

is evident for both the low- and high-flux states with the archival 1ES 2344+514 data, and compared with one-zone SSC modeling of similar moderate-flux level flares in the HBLs 1ES 1959+650 (Tagliaferri et al. 2008), 1ES 0806+524 (Acciari et al. 2009), and 1ES 1101-213 (Aharonian et al. 2007). A detailed study of the SSC model parameter space (e.g., Tavecchio et al. 1998) is not pursued here due to sparseness in the SED coverage and degeneracy between model parameters. The simple one-zone SSC modeling presented here adequately describes the data, however, further optical, X-ray, and VHE γ-ray observations of 1ES 2344+514 simultaneous with *Fermi* LAT promise to offer stronger constraints to emission models.

8. CONCLUSION

In this paper, a ∼4 month long VHE γ-ray and X-ray observing campaign of 1ES 2344+514 revealed significant flux variability on ∼1 day timescales. In particular, flux doubling between nights is evident in both the X-ray and VHE γ-ray bands in 2007 December, with the highest ever X-ray flux measured from 1ES 2344+514 on 2007 December 8. Evidence of correlated nightly X-ray flux and VHE γ-ray flux variability is shown, as generally found in the well-studied HBLs Mrk 501 (Krawczynski et al. 2000), Mrk 421 (Fossati et al. 2008), and 1ES 1959+650 (Krawczynski et al. 2004), however, so-called orphan flares of increased flux in one energy band and not the other have also been observed (e.g., (Błażejowski et al. 2005; Krawczynski et al. 2004)). For these campaigns sparse temporal sampling and insufficient VHE sensitivity to short timescale variability limited any statements on a linear or quadratic relationship between VHE and X-ray flux expected under various SSC scenarios during rising or decaying flares (Fossati et al. 2008). The 1ES 2344+514 data presented here represent the first contemporaneous multiwavelength campaign of the object from UV to VHE γ-rays, but are similarly restricted by sparse temporal sampling and broadband coverage in the SEDs. Applying a simple one-zone SSC model reasonably describes the data, and is consistent with past modeling of the object and other HBLs. Further optical, X-ray, and VHE γ-ray observations of 1ES 2344+514 simultaneous with *Fermi* LAT in the HE γ-ray band promise to offer stronger constraints to emission models and high sensitivity broadband measurements of high-flux state flaring events.

This research is supported by grants from the U.S. Department of Energy, the U.S. National Science Foundation, and the Smithsonian Institution, by NSERC in Canada, by STFC in the UK and by Science Foundation Ireland. Special acknowledgment to the *Swift* and *RXTE* teams for the support of these observations.

REFERENCES

Abdo, A. A., Ackermann, M., Ajello, M., et al. 2010, ApJS, 188, 405
Acciari, V. A., Aliu, E., Arlen, T., et al. 2009, ApJ, 690, L126
Acciari, V. A., Beilicke, M., Blaylock, G., et al. 2008, ApJ, 679, 1427
Aharonian, F. 2000, New Astron., 5, 37
Aharonian, F., Akhperjanian, A., Barrio, J., et al. 2001, A&A, 370, 112
Aharonian, F., Akhperjanian, A. G., Bazer-Bachi, A. R., et al. 2007, A&A, 470, 475
Aharonian, F., Akhperjanian, A., Beilicke, M., et al. 2004, A&A, 421, 529
Albert, J., Aliu, E., Anderhub, H., et al. 2007, ApJ, 662, 892
Blandford, R. D., & Königl, A. 1979, ApJ, 232, 34
Błażejowski, M., Blaylock, G., Bond, I. H., et al. 2005, ApJ, 630, 130
Böttcher, M., & Chang, J. 2002, ApJ, 581, 127
Bradt, H. V., Rothschild, R. E., & Swank, J. H. 1993, A&AS, 97, 355
Burrows, D., Hill, J. E., Nousek, J. A., et al. 2005, Space Sci. Rev., 120, 165
Catanese, M., Akerlof, C. W., Badran, H. M., et al. 1998, ApJ, 501, 616
Coppi, P. S. 1992, MNRAS, 258, 657
Daniel, M. K., et al. 2007, in Proc. 30th ICRC, Merida, Mexico, 283
Elvis, M., Plummer, D., Schachter, J., & Fabbiano, G. 1992, ApJS, 80, 257
Falomo, R., & Kotilainen, J. K. 1999, A&A, 352, 85
Fitzpatrick, E. 1999, PASP, 111, 63
Fossati, G., Buckley, J. H., Bond, I. H., et al. 2008, ApJ, 677, 906
Franceschini, A., Rodighiero, G., & Vaccari, M. 2008, A&A, 487, 837
Gehrels, N., Chincarini, G., Giommi, P., et al. 2004, ApJ, 611, 1005
Giommi, P., Padovani, P., & Perlman, E. 2000, MNRAS, 317, 743
Giroletti, M., Giovannini, G., Taylor, G. B., & Falomo, R. 2004, ApJ, 613, 752
Godambe, S. V., Rannot, R. C., Baliyan, K. S., et al. 2007, J. Phys. G: Nucl. Part. Phys., 34, 1683
Gould, R. J., & Schréder, G. P. 1967, Phys. Rev., 155, 1408
Gupta, A. C., Fan, J. H., Bai, J. M., & Wagner, S. J. 2008, AJ, 135, 1384
Hillas, A. M. 1985, in Proc. 19th ICRC, La Jolla, USA, 3, 445
Hofmann, W., Jung, I., Konopelko, A., et al. 1999, Astropart. Phys., 12, 135
Holder, J., Atkins, R. W., Badran, H. M., et al. 2006, Astropart. Phys., 25, 361
Jahoda, K., Swank, J. H., Giles, A. B., et al. 1996, Proc. SPIE, 2808, 59
Kalberla, P. M. W., Burton, W. B., Hartmann, D., et al. 2005, A&A, 440, 775
Krawczynski, H., Carter-Lewis, D. A., Duke, C., et al. 2006, Astropart. Phys., 25, 380
Krawczynski, H., Coppi, P. S., Maccarone, T., & Aharonian, F. A. 2000, A&A, 353, 97
Krawczynski, H., Hughes, S. B., Horan, D., et al. 2004, ApJ, 601, 151
Mannheim, K. 1993, A&A, 269, 67
Mücke, A., & Protheroe, R. J. 2001, Astropart. Phys., 15, 121
Nilsson, K., Pursimo, T., Takalo, L. O., et al. 1999, PASP, 111, 1223
Perlman, E. S., Stocke, J. T., Schachter, J. F., et al. 1996, ApJS, 104, 251
Poole, T. S., Breeveld, A. A., Page, M. J., et al. 2008, MNRAS, 383, 627
Rector, T. A., Gabuzda, D. C., & Stocke, J. T. 2003, AJ, 125, 1060
Schroedter, M., Badran, H. M., Buckley, J. H., et al. 2005, ApJ, 634, 947
Stevens, J. A., & Gear, W. K. 1999, MNRAS, 307, 403
Tagliaferri, G., Foschini, L., Ghisellini, G., et al. 2008, ApJ, 679, 1029
Tavecchio, F., Maraschi, L., & Ghisellini, G. 1998, ApJ, 509, 608
Tramacere, A., Giommi, P., Massaro, E., et al. 2007, A&A, 467, 501
Vaughan, S., Edelson, R., Warwick, R. S., Uttley, P., et al. 2003, MNRAS, 345, 1271
Weekes, T. C., Badran, H., Biller, S. D., et al. 2002, Astropart. Phys., 17, 221
Xie, G. Z., Zhou, S. B., Dai, B. Z., et al. 2002, MNRAS, 329, 689